The Molecular Transport Behavior of CO_2 in Ionic Polyimides and Ionic Liquid Composite Membrane Materials

Joanna Szala-Bilnik, Asghar Abedini, Jason E. Bara, C. Heath Turner*

Department of Chemical and Biological Engineering, The University of Alabama, Tuscaloosa, Alabama, USA 35487-0203

Abstract

Ionic polyimides (i-PI) are a new class of polymer materials that are very promising for CO_2 capture membranes, and recent experimental studies have demonstrated their enhanced separation performance with the addition of imidazolium-based ionic liquids (ILs). However, there is very little known about the molecular-level interactions in these systems, which give rise to interesting gas adsorption and diffusion characteristics. In this study, we use a combination of Monte Carlo and molecular dynamics simulations to analyze the equilibrium and transport properties of CO_2 molecules in the i-PI and i-PI+IL composite materials. The addition of several different common ILs are modeled, which have a plasticization effect on the i-PI, lowering the glass transition temperature (T_g). The solubility of CO_2 strongly correlates with the T_g, but the diffusion demonstrates more unpredictable behavior. At low concentrations, the IL has a blocking effect, leading to reduced diffusion rates. However, as the IL surpasses a threshold value the relationship is inverted, and the IL has a facilitating effect on the gas transport. This behavior is attributed to the simultaneous contributions of the increased i-PI plasticization at higher IL concentrations (facilitating gas hopping rates from cavity-to-cavity) and the increased IL continuity throughout the system, enabling more favorable transport pathways for the CO_2 diffusion.

*Corresponding author contact information
hturner@eng.ua.edu
205-348-1733 (ph)

1. Introduction

The removal of CO_2 from both pre- and post-combustion gas streams is an important industrial need, due to concerns of environmental impacts and global warming. Some of the most common applications of CO_2 separation technologies include H_2/CO_2 separation in the pre-combustion stage of integrated coal gasification processes, CO_2/N_2 separation of post-combustion emissions, or CO_2/CH_4 separation for natural gas sweetening.[1-4] However, the current solvent-based CO_2 separation methods (e.g., aqueous monoethanolamine (MEA)) still suffer from high-energy demands, corrosivity, volatility, and toxicity issues.[5]

Polymer membranes may provide a viable alternative for CO_2 separation, considering the low maintenance, minimal energy demands, compact design, and relatively low cost.[2, 6] However, there are several other factors that must also be considered, such as stability in harsh environments and the inherent tradeoff between selectivity and permeability.[7] In order to mitigate some of these practical challenges, composite and mixed-matrix polymer membranes are seen as promising candidates.[8]

Polyimides (PIs) are useful materials for a variety of applications (electrical devices, aerospace materials, optical applications, etc.), due to their good thermal stability, mechanical strength, optical transparency and solvent solubility. Among these PI materials, several have demonstrated high gas permeability or CO_2 selectivity, such as those synthesized from bulky dianhydrides such as 4,4-hexafluoroisopropylidene diphthalic anhydride (6FDA) or bulky diamines 2,3,5,6-tetramethyl-1,4-phenylene diamine (TeMPD).[9, 10] In addition to these materials, polymerized ionic liquids (poly(IL)s) have attracted scientists' attention.[11, 12] Ionic liquids (ILs) possess relatively

good thermal stability, low volatility, and they have the ability to dissolve a wide range of organic molecules.[13] They are also considered to be environmentally benign alternatives to many industrial organic solvents. Furthermore, poly(IL)s or polymer systems with supported ILs can be designed to leverage the advantages of both ILs and membranes, thereby circumventing some of the limitations of traditional membrane materials.[14-16]

Recently, several computational and experimental studies have been conducted to study the adsorption and diffusivity of CO_2 in composite membranes, both computational and experimental.[17-25] Budhathoki et al.[18] used molecular dynamics (MD) simulations to study CO_2 solubility selectivity, diffusion selectivity and permselectivity from mixtures of CO_2/CH_4 and CO_2/H_2 within the IL 1-butyl-3-methylimidazolium bis(trifluoromethylsulfonyl)imide, $[C_4mim][Tf_2N]$, confined within graphite nanopores of 2 - 5 nm in diameter. These studies showed an improvement in the permselectivity, but a decrease of the diffusivity compared to the bulk IL. Song et al.[20] computationally investigated the IL/poly(vinylidene fluoride) (PVDF) membrane with IL weight fractions of 0 %, 10 %, 20 % 30 %, 40 %, 50% and 100% (pure). Within the PVDF, the ILs were found to aggregate, leading to the gradual formation of continuous ionic channels as a function of the IL loading. These continuous ionic channels enhanced the CO_2 diffusion, but this was only possible with high IL concentrations. Li et al.[26] have also reported the advantages of adding ILs to polymerized ILs with respect to CO_2 separation in their experimental studies. An increase in $[C_4mim][Tf_2N]$ concentration within a poly([vbim][Tf_2N])–$[C_4mim][Tf_2N]$ composite membrane resulted in an increase in solubility, diffusivity, and permeability of CO_2 and N_2, but the IL addition does not change the corresponding CO_2/N_2 selectivities. Kanehashi et al.[27] studied composite

membranes composed of glassy fluorine-containing polyimide (PI) containing up to 81 wt% of [C_4mim][Tf_2N] and discovered that the gas permeability increased from 35.5 barrers to 501 barrers in the membrane, corresponding to an IL content of 51 to 81 wt%, respectively. This increase in gas permeability was attributed to the increase in gas diffusivity. Additionally, Chen et al.[21] synthesized a 1-ethyl-3-methylimidazolium tetracyanoborate [C_2mim][$B(CN)_4$]/PVDF composite membrane and investigated the effect of IL concentration on CO_2 separation performance. It was found that the CO_2 permeability increases with increasing ILs content, and the [C_2mim][$B(CN)_4$]/PVDF membrane has a CO_2 permeability of 1595 barrers with a CO_2/N_2 selectivity of 37.5. The CO_2/N_2 performance surpasses the 2008 Robeson upper bound.

The transport properties of IL/sulfonated polyimide (SPI) composite membranes for CO_2 separation have been explored by Ito et al.,[22] with a focus on the material nanostructure. The diffusion coefficients of CO_2 abruptly increase with increasing IL content in the [C_4mim][Tf_2N]/SPI composite membranes, which coincide with a change from an isolated to a continuous IL-rich nanostructure. On the other hand, the solubility selectivity of CO_2 in the [C_4mim][Tf_2N]/SPI composite membranes exhibits no relation to the IL content. Consequently, the permeation coefficient of the membranes increases with respect to the IL content, but the separation factor is unaffected.

Directly related to our current investigation, the Bara group[23] experimentally studied a neat i-PI and an i-PI + IL composite, and they found an increased gas permeability, from 0.88 barrers to 20.4 barrers for CO_2 and from 0.03 to 0.80 barrers for CH_4, respectively, with the gas solubility essentially unchanged. This is the same system

that we are currently modeling, in order to establish a deeper understanding of the molecular mechanisms underlying the transport phenomena.

Some new, three-component mixed-matrix membranes, cross-linked poly(IL) + IL + zeolite,[25] have shown good CO_2 permeability and CO_2/CH_4 selectivity. There are many examples of composite membranes showing improved CO_2 permeability and selectivity relative to the pure polymer, but the overall CO_2 separation performance depends on the combination of the ILs and polymer. Unfortunately, there is very little fundamental guidance with respect to predicting and selecting the appropriate IL/polymer combination from the vast experimental parameter space that is available.

In order to develop a clearer picture of these composite systems, and simultaneously build upon the results that we have already experimentally obtained,[23] we are investigating the transport behavior of gas molecules (primarily CO_2) within i-PI and i-PI + IL composite materials. These i-PI polymers incorporate ionic liquid cations in the backbone separated by an organic linker (PMDA, in our case) in the neat membrane; a counter ion ($[Tf_2N^-]$, $[PF_6^-]$ or $[BF_4^-]$) is used to balance the charge. In the i-PI+IL composite materials, $[C_4mim^+]$-based ILs with these same corresponding anions are added to the system at various loadings. In our previous work,[28, 29] we focused on gas ($CO_2/CH_4/N_2$) adsorption and selectivity within i-PI polymers, as well as i-PI + IL composites. Depending upon the specific IL used, vastly different adsorption and selectivity properties emerge. The results vary non-linearly with respect to the IL loading, but we found a strong correlation between the calculated surface area and the gas solubility. Whereas our previous work focused on the adsorption selectivity, we now shift our focus to explore the gas diffusion behavior within these same i-PI + IL materials,

in order to develop a more comprehensive picture of the tradeoff between the selectivity and permeability.[7]

We are exploring a combination of i-PIs with ILs, in order to take advantage of the significant fractional free volume (FFV) of the i-PIs (due to their structural rigidity) and the tunable selectivity and induced plasticity provided by the ILs. Our simulation results indicate that there is a nonlinear correlation between the IL concentration and the transport behavior. When the IL concentration is low, there is a blocking effect that impedes the CO_2 transport, whereas at higher concentrations of IL (>30 mole%), the percolation of the IL through the system leads to enhance gas transport. Furthermore, we characterize the properties of these systems by calculating the glass transition temperature (T_g), FFV and internal surface area. We find linear increases in the gas solubility with respect to the T_g, but the CO_2 diffusion coefficient is mainly controlled by the nonlinear (blocking versus facilitating) effect of the IL molecules, versus the induced changes in the T_g or the FFV. Additionally, the T_g of the composite systems appears to be related to the viscosity of the neat ILs added to the system.

2. Simulation Details

The structure of our i-PI monomer is presented in Figure 1, along with key atomic labels. In total, 200 monomers were used to build these polymers in a cubic periodic simulation cell, and a detailed description of our polymerization procedure can be found in our previous papers.[28, 29] Three neat i-PI systems are studied, each corresponding to a different counter ion ($[Tf_2N^-]$, $[PF_6^-]$ or $[BF_4^-]$), as well as seven composite i-PI + IL systems, each with different concentrations (10 mole%, 30 mole% and 50 mole%) of IL

additives: ([C_4mim][Tf_2N], [C_4mim][PF_6], or [C_4mim][BF_4]). In order to initially relax the systems, we increased the temperature to 2000 K in the NVT ensemble, followed by an NPT simulation at a pressure corresponding to the preceding NVT simulation. Then, alternating stages of NVT/NPT were applied until the systems were gradually cooled to the desired temperature of 294 K and a pressure of 1 bar. After relaxation, CO_2 was adsorbed into the different samples using grand canonical Monte Carlo (GCMC) simulations, corresponding to a pressure of 1 bar and a temperature of 294 K with Cassandra,[30, 31] according to our previous multi-step procedure (to improve sampling).[28,29] In brief, the GCMC simulations (3 x 10^6 steps) were alternated with cycles of MD simulations (1 ns in duration, each). These MC/MD cycles were repeated to until a stable number of adsorbed CO_2 molecules was obtained. After saturation (typically requiring 15 MC/MD cycles), the systems were relaxed for an additional 20 ns of MD simulation. During the GCMC stages, the polymer and IL molecules were held rigid, while full relaxation was allowed during MD stages.

To study the transport mechanism of CO_2 gas molecules in the i-PI and i-PI + IL systems, long-time simulations are required (approximate 150 ns of MD simulation). All systems were simulated at conditions of 294 K and 1 bar. The MD simulations were performed with the GROMACS 5.0 simulation package.[32] The Lennard-Jones potential and electrostatic interactions were calculated with a cutoff distance of 1.4 nm, and the smooth particle mesh Ewald sum (SPME)[33] method was implemented for long-range electrostatic interaction with 0.16 nm of Fourier spacing. The Nose−Hoover thermostat[34] was used to maintain the temperature, the Parrinello−Rahman[35] barostat was used to maintain the pressure, and the time step was 1 fs. The i-PI was modeled using the OPLS-

AA force field[36] with the partial charges estimated previously,[29, 37] based on electronic structure calculations. As in our previous work, the force filed parameters for the ionic liquids (IL) were taken from Lopez et al.,[38-41] and the TraPPE force field was used for CO_2.[42-44] The Lorentz–Berthelot mixing rules were used for cross-term interactions.

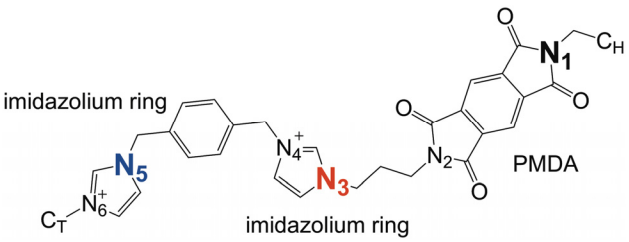

Figure 1. The structure of our i-PI monomer with the key atomic labels indicated.

To estimate T_g the densities of the systems were calculated and analyzed at temperatures ranging from 294 to 900 K. Our systems were initially heated up to 2000 K and then slowly cooled down in stages of NVT and NPT conditions to the desired temperature. After equilibration, the density was averaged over a period of 20 ns at each temperature to obtain the reported density, which is then used to estimate the T_g. To estimate the diffusion coefficient (D^{MSD}), the mean squared displacement (MSD) of the CO_2 molecules (center of the mass) was calculated over a timespan of 150 ns. The diffusion coefficient was obtained using the Einstein relation corresponding to the linear regime, but even with extended trajectories, the slow transport can be problematic.

3. Results and Discussion

3.1 Structural and equilibrium properties of i-PI and i-PI + IL polymers

It is generally known that gas transport through polymer membranes is strongly influenced by the underlying structure and dynamics of the polymer.[2, 3, 45] For instance, if

the structure is rigid, the diffusion of the gas molecules in the membrane can be significantly impacted, since the diffusion pathways often involve concerted motions of the polymer backbone.[46] With regards to the structural details, the size of the voids as well as their connectivity can also have a strong influence on the gas diffusion behavior. We begin with an analysis of the equilibrium structural properties, including the predicted glass transition temperature. For convenience, the different systems follow the naming convention listed in Table 1.

Table 1. Naming convention for i-PI and i-PI + IL systems. The predicted glass transition temperatures (T_g) are indicated, as well as the surface area and FFV.[28, 29] Errors for T_g, FFV and surface area are below 5%, 6% and 10%, respectively.

Polymer system	Short name	T_g, K	Surface area, $m^2\ cm^{-3}$	FFV
Neat i-PI Tf_2N	N Tf_2N	428	303.9	0.305
Neat i-PI PF_6	N PF_6	355	457.6	0.297
Neat i-PI BF_4	N BF_4	378	390.3	0.303
i-PI + 10% IL [BMIM][Tf_2N]	10 Tf_2N	405	307.8	0.311
i-PI + 30% IL [BMIM][Tf_2N]	30 Tf_2N	390	280.2	0.311
i-PI + 50% IL [BMIM][Tf_2N]	50 Tf_2N	388	267.3	0.310
i-PI + 10% IL [BMIM][PF_6]	10 PF_6	350	441.7	0.305
i-PI + 30% IL [BMIM][PF_6]	30 PF_6	345	413.8	0.305
i-PI + 50% IL [BMIM][PF_6]	50 PF_6	340	385.4	0.310
i-PI + 50% IL [BMIM][BF_4]	50 BF_4	358	325.1	0.303

In our previous work, we performed a thorough analysis of the structural properties of these same i-PI + IL systems, including the surface area and fractional free volume (FFV).[28, 29] These structural properties were calculated using the Gelb and Gubbins approach[47], which include all atomic sites during the analysis, with the assigned Lennard-Jones diameters used to define the location of the atomic surfaces and volumes.

As summarized in Table 1, a higher surface area was found for the neat i-PI as compared to the i-PI+IL composite. When comparing polymers composed of different anions, the highest surface area was found for the [PF_6^-] anion and the lowest for [Tf_2N^-]. Our studies have also revealed that CO_2 solubility strongly correlates with the calculated surface area, and the highest solubility was found for the [PF_6^-] anion (but regardless of the anion, the neat polymers still showed higher solubility). In contrast to the surface area, the FFV was higher for the i-PI + IL composite than for the neat i-PI (with the same anion). Also, the highest FFV was found for the [Tf_2N^-] anion, which has the lowest surface area. In addition to these previous structural properties, here we have calculated the glass transition temperatures (T_g) for all membranes, as summarized in Table 1. The thermodynamic data used to generate these results are included in the Supporting Information.

The glass transition temperature is the highest for the neat i-PI, and it decreases with respect to the addition of the IL, regardless of the anion type. This effect can be explained by plasticization of the polymer in the presence of ILs. Kanehashi et al. found a similar effect in their studies of neat PI (6FDA-TeMPD) and PI with the different concentrations (from 9 to 83 wt%) of [bmim][Tf_2N].[27] The T_g for the neat polymer was 697 K with an FFV equal to 0.186. These values decrease with the increase in IL loading, reaching a T_g of 330 K and an FFV of 0.126 for the membranes with 83 wt% IL. The Bara group[48] investigated the thermal behaviors of imidazolium polyimide - ionenes with several different counter ions (including [PF_6^-], [BF_4^-], and [Tf_2N^-]) and several different linkers (including PMDA). In the contrast to our studies, the lowest T_g (308 K) was found for the system with [Tf_2N^-] and the highest for [BF_4^-] (450K). However, the experimental

thermogravimetric analysis data reveals that the [Tf_2N^-] anion resisted degradation more than the [PF_6^-] and [BF_4^-] derivatives, and this could strongly affect the results. Also, it was noted that while the [Tf_2N^-] derivatives exhibit a more rapid decrease in mass, the breakdown of the [PF_6^-] and [BF_4^-] systems occurs over a greater temperature range.

The trends of the T_g behavior show strong correlations with the calculated surface area, as presented in Figure 2. There is some correlation with the FFV, but due to the large statistical uncertainty compared to the trends in the values, the correlation is not significant.

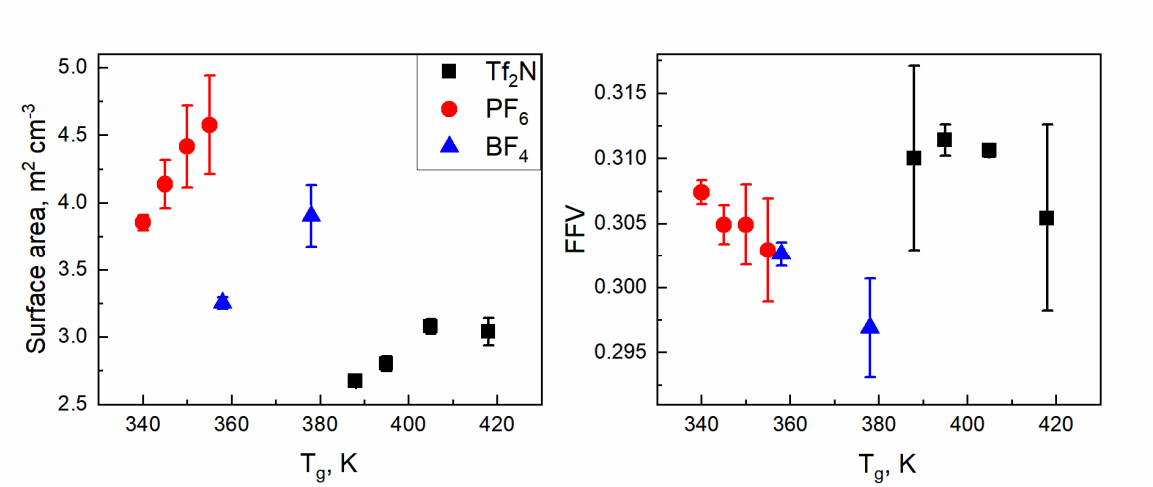

Figure 2. Surface area (left) and fractional free volume (FFV) (right) vs. the glass transition temperature (T_g). Error bars are calculated from two or three different independent simulation runs.

The T_g is the lowest for the [PF_6^-] composite membrane, and the highest for [Tf_2N^-]. Furthermore, the T_g depends more on the anion type than on the amount of the IL added. The experimental viscosity of the bulk ILs used in our studies follows the trend [PF_6^-] > [BF_4^-] > [Tf_2N^-],[49-51] and this correlates quite well with the i-PI systems, with the lowest T_g's for [PF_6^-]-based polymers, and the highest T_g's for the [Tf_2N^-]-based systems.

Additionally, with the same anion, the T_g decreases with the increase in the IL loading, which can be simply explained by the lower T_g of the bulk IL (versus the neat polymer).

With the increase of T_g, the calculated surface area tends to decrease, and this is likely due to changes in the polymer-polymer interactions in the system. For instance, with a decrease in surface area, there are likely more regions of intermolecular contact (and attractive interactions) reducing the mobility of the polymer, and thus increasing the T_g. To quantify this, the radial distribution functions, g(r), between different sites of the polymer backbone (Figure S-1 of the Supporting Information) reveal that in the polymer systems with 50 mole% IL, the peak positions are shifted to longer distances as compared to the neat polymer. This suggests an expansion of the polymer and weaker interactions between neighboring polymer segments.

Our previous modeling studies showed that solubility is strongly correlated with the surface area.[29] Therefore, since the surface area strongly correlates with T_g, the correlation between solubility and T_g is a natural outcome (Figure 3). Similar to our work, Kanehashi et al.[27] also found an increase in gas solubility with respect to an increase in the T_g for their 6FDA-TeMPD PI + $[C_4mim][Tf_2N]$ composite membrane. In general, the polymer T_g reflects the unrelaxed excess free volume that is closely related with the Langmuir adsorption.[52, 53] Additionally, the decrease in gas solubility with the increase in IL loading may be ascribed to the reduction of the unrelaxed volume of polymer due to the IL-induced plasticization[52, 53]. For instance, in our previous study,[29] we tracked the cavity-size distribution in the system with respect to the IL loading. As the IL loading increased, the larger voids (>3 Å diameter) in the composite material were diminished.

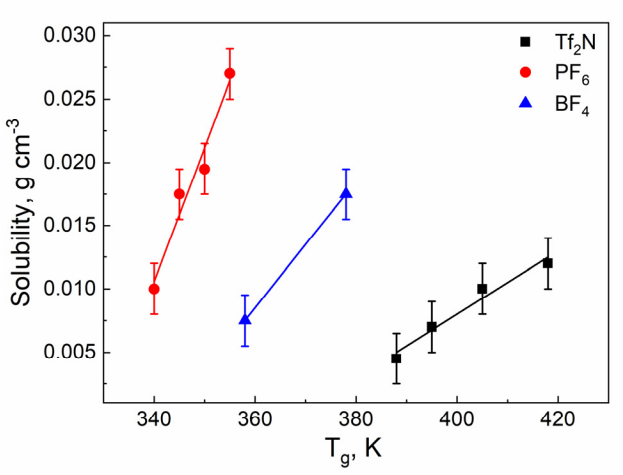

Figure 3. The predicted CO_2 solubility as a function of T_g for the different i-PI+IL systems.

In order to understand the preferred locations of the gas molecules, the radial distribution functions (RDFs) between CO_2 and different IL and i-PI sites are analyzed, including: N atoms of the polymer backbone (N1 and N2 correspond to the linker, while N3 and N4, N5 and N6 are located within the cation rings); N, B or P atom (central atom) of the anion; and NA and CR atoms of the cation ring. The RDFs for the PF_6-based polymers are presented in Figure 4. The RDFs for all systems are shown Figure S2 and Figure S3 in the Supporting Information.

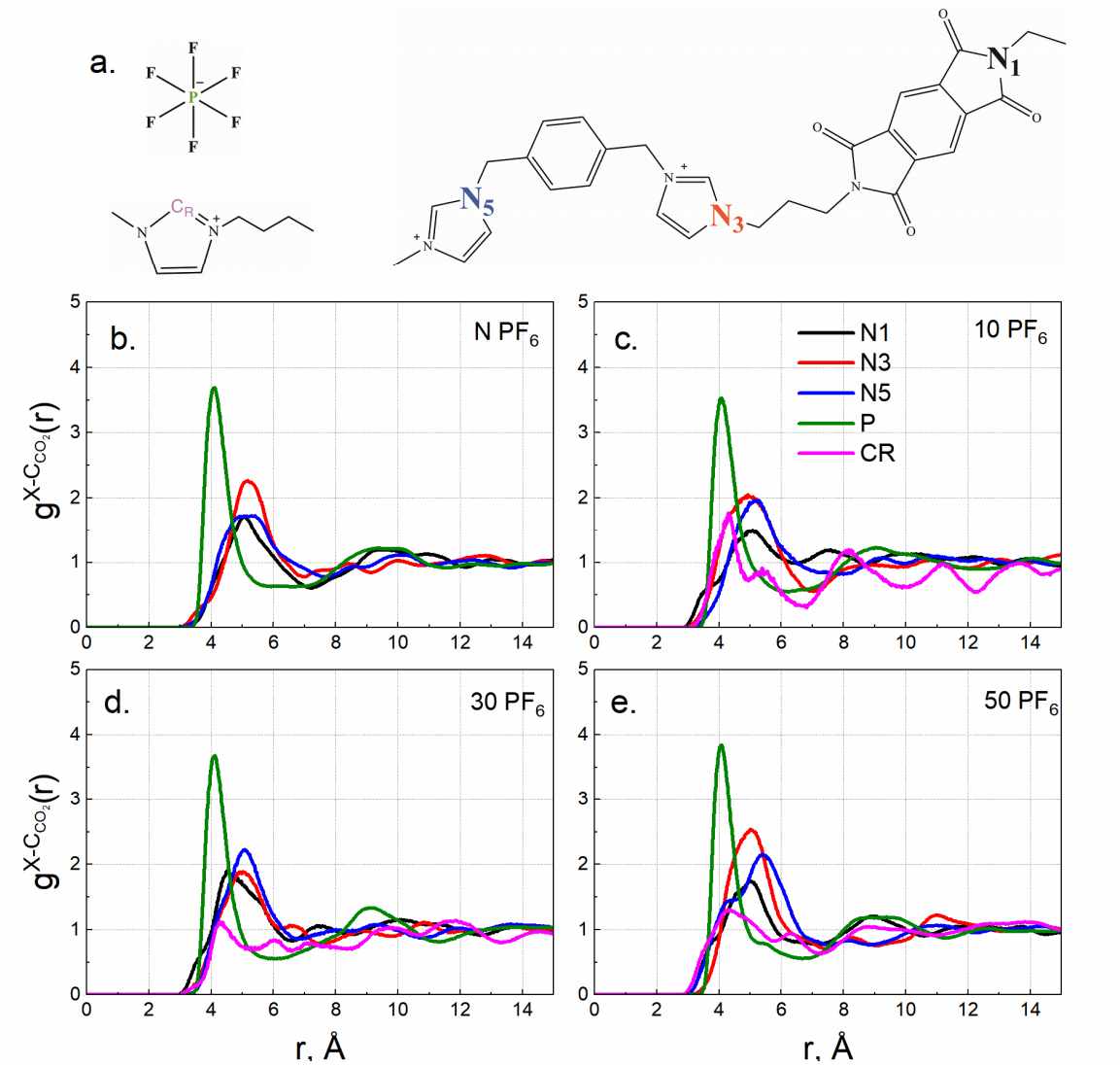

Figure 4. The RDFs between CO_2 and different sites of the IL and i-PI. The chosen sites are illustrated in (a) with the colors corresponding to the colors in the RDF plots. The RDFs corresponding to different [PF_6^-]-based systems are shown in (b) N PF_6, (c) 10 PF_6, (d) 30 PF_6, and (e) 50 PF_6.

In all systems, the CO_2 molecules are found to be more strongly associated with the anion than with the polymer backbone. Similar behavior was found for the [BF_4^-]-based composite systems. In the case of [Tf_2N^-] some differences were found. The distance between the anion and gas molecules is shorter than between the polymer and CO_2, but the affinity between the anion and CO_2 and polymer and CO_2 are similar. Additionally, with the increase in cation concentration, the association between it and

CO_2 is increasing. This effect was not found in any other systems and can be related to lower solubility of CO_2 in this system.

3.2. CO_2 Transport Behavior

In order to more clearly understand the transport behavior of the CO_2 molecules in the different polymer systems, the diffusion coefficient has been calculated using the mean squared displacement (MSD). The exemplary curves are presented in Figure 5, and the diffusion coefficients for all systems are collected in Table 2.

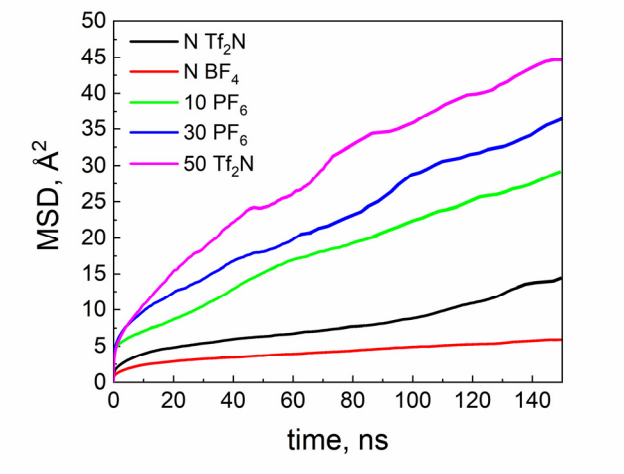

Figure 5. Mean squared displacements (MSD) of CO_2 for representative neat i-PI and i-PI+IL composite polymers.

Table 2. The diffusion coefficient of CO_2 in all systems calculated from the mean squared displacement (MSD), along with standard deviations calculated from independent runs.

System	D^{MSD}, 10^{-9} cm^2 s^{-1}
N Tf_2N	2.30 ± 0.40
N PF_6	4.36 ± 0.89
N BF_4	0.80 ± 0.50
10 Tf_2N	1.10 ± 0.87
30 Tf_2N	2.40 ± 0.84
50 Tf_2N	7.63 ± 1.21

10 PF_6	1.50 ± 0.34
30 PF_6	2.70 ± 0.22
50 PF_6	9.80 ± 0.20
50 BF_4	4.60 ± 0.57

Although the MSDs curves were calculated using 150 ns of simulation time, the diffusion coefficients still have moderate statistical error. In the Supporting Information, we summarize the diffusion coefficients of CO_2 in similar polymeric materials and pure ionic liquids found in the literature. In general, the diffusion coefficients reported[11, 26, 27, 54-57] are much higher than in our studies, but there are some important points to note. For instance, the Bara group[23] tested systems similar to our N Tf_2N and composite 50 Tf_2N materials, and they report CO_2 diffusivities of 3.08 x 10^{-9} cm^2 s^{-1} and 7.56 x 10^{-8} cm^2 s^{-1} in the neat and composite systems, respectively. The simulated and experimental diffusion coefficients in the neat systems are similar, but in the composite membranes, there are larger differences. Additionally, the experimental results showed slightly lower solubility in the composite material than in neat membrane, while in our studies, it is more than two times smaller in the composite. Overall, both simulation and experiment provide qualitatively consistent trends that the CO_2 permeability is higher in the composite membrane than in the neat system.

Li et al.[26] showed that the diffusion coefficient increases with the increase in the concentration of the free IL dispersed in the polymerized ILs. A similar relationship was found by Kanehashi et al.[27] However, in the Kanehashi's study, a significant drop in the diffusion coefficient was observed at low IL concentrations, with a minimum diffusion coefficient found at around 30 wt% IL concentration. Beyond this concentration, a steady

increase in the diffusion coefficient was observed. In our studies, similar decreases in the diffusion coefficient were found with the addition of 10 mole% IL, whereas the diffusion coefficient increases when the IL concentration moves beyond this value.

Although several of the trends of the diffusion coefficient were consistent with previous studies, our values are much lower than those reported in the literature. In order to investigate this further, we performed more detailed analyses of the CO_2 transport. To this end, we tracked the distance between the relative positions of the CO_2 molecules as a function of time in all systems. Several randomly-chosen CO_2 trajectories in the 50 Tf_2N system are presented in Figure 6.

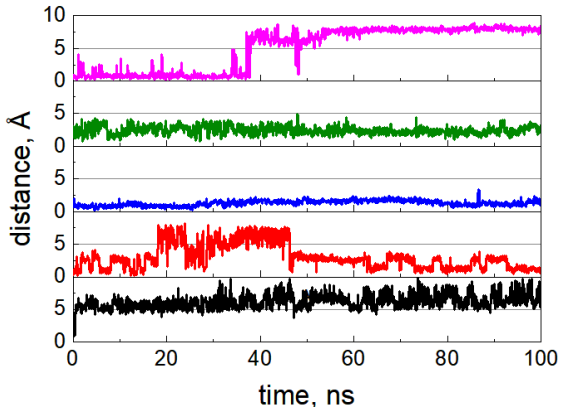

Figure 6. The relative distance from the initial positions of CO_2 molecules as a function of time in the 50 Tf_2N system. Five randomly choosen molecules are displayed (corresponding to approximately 20% of the total adsorbates). Each color corresponds to a different CO_2 molecule.

As can be seen in Figure 6, the CO_2 molecules tend to remain within 0 to 2 Å of their original positions, even after a significant amount of time. The molecules only intermittently are able to jump to a new location (void) within the polymer. All systems were further analyzed with in-house scripts to more precisely describe the overall statistical behavior of the CO_2 molecules. Table 3 presents the percentage of the

molecules that are able to escape within the simulation timespan of 150 ns to distances greater than 2 Å (criterion G2), 5 Å (criterion G5) or 10 Å (criterion G10) from the initial position. The criterion G2_2 is the percentage of the molecules that stay within a distance of 0 to 2 Å between consecutive time steps (1 fs). All values are averaged over all molecules and all configurations.

The hopping probability was also estimated from the statistical distribution of CO_2 lifetime within particular regions. For the neat systems, the probability of an individual CO_2 molecule to escape from a cavity within the simulation timespan of 150 ns (i.e., jump more than 2 Å) is around 0.2; this probability drops to 0.04 if temporary in-out jumps are ignored. In the composite membranes, these values tend to be approximately twice as large (0.4 and 0.1, respectively).

Table 3. The percentage of the molecules in criterion G2, G5, G10 and G2_2 calculated within a time of 150 ns.

	G2	G5	G10	G2_2
N Tf_2N	38.3	19.2	0.2	99.96
10 Tf_2N	28.9	10.9	0.6	99.81
30 Tf_2N	28.8	8.7	0.1	99.82
50 Tf_2N	40.6	21.3	4.8	99.83
N PF_6	16.4	11.4	4.4	99.88
10 PF_6	30.6	12.5	1.9	99.62
30 PF_6	30.8	13.1	3.3	99.62
50 PF_6	30.6	13.0	0.8	97.78
N BF_4	21.7	0.5	0.1	99.99
50 BF_4	31.2	6.2	0.7	99.84

In all systems, the CO_2 molecules spend an average of 71.2 ns within the range of 0 to 2 Å from their original positions. If the distance criterion is extended to 5 Å, the

average duration time increases to 88.3 ns. These long residence times are separated by a few large transitions, indicative of a hopping mechanism. However, it is also important to emphasize that there are significant differences between the neat and composite membranes. Although, the diffusion of CO_2 in all polymers is restricted, the duration between large jumps is around 10% less in the composite systems than in the neat systems. This behavior is consistent with the higher diffusion coefficients of CO_2 in the i-PI+IL composite systems versus the neat i-PI polymer.

The diffusion coefficients of CO_2 in neat and composite membranes as a function of IL concentration and predicted glass transition temperature (T_g) are presented in Figure 7 for comparison. The diffusion coefficient in the neat i-PI is significantly slower than in the composite membranes with the highest IL content. However, the addition of a small amount (around 10 mole%) of IL to the system decreases the diffusion coefficient.

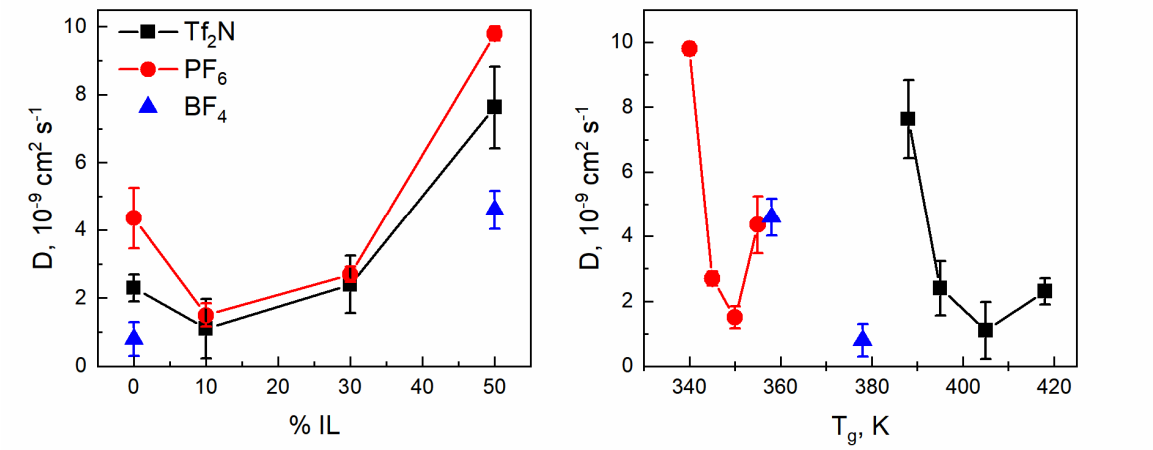

Figure 7. The diffusion coefficient in the i-PI+IL systems as a function of IL loading (left) and T_g (right).

Figure 7 shows that diffusion is more strongly related to the amount of IL added than to the specific anion. The [PF_6^-]-based polymers have the lowest T_g and the [Tf_2N^-]-

based polymers have the highest T_g, but the highest diffusion coefficients were found for the systems with 50 mole% of IL added, regardless of the anion (although [PF_6^-] shows some advantages).

As shown in Table 1, polymers with IL added have lower glass transition temperatures than the neat i-PI. This plasticization behavior is generally accompanied by different transport phenomena: facilitating versus blocking effects.[60] The facilitating effect leads to an increase in the gas diffusivity, while the blocking effect causes a decrease in the diffusivity and solubility. Within this framework, the decrease in the gas diffusivity in our systems with low concentrations of IL is related to the pore blocking effect. The gas diffusion route is impeded by the dispersed IL at the low concentrations without a significant effect on the T_g (polymer mobility) of the system. By contrast, the gas diffusivity significantly increases as the concentration of IL is elevated to higher levels. This behavior emerges as the plasticization of the i-PI begins to occur, induced by higher IL concentrations. Therefore, it seems that a threshold concentration of IL must be added to impart a meaningful plasticization effect enabling the CO_2 molecules to more easily jump through the membrane. Some authors have suggested[27, 57] that the IL domain drives the diffusion of CO_2 in similar composite membranes, and this may also be a reasonable depiction of our system. In all systems, the CO_2 molecules are found to be more strongly associated with the anion than with the polymer backbone (Figure 4). Similar behavior was found for the other composite systems. Thus, the suggested gas diffusion pathway via the IL domain in the composite materials (previously suggested by others[27, 60]) seems to also be consistent with our system.

In contrast to the solubility (Figure 3), the diffusion coefficient does not linearly correlate with the FFV or surface area (Figure S4 in Supporting Information). The changes in the diffusivity can be more clearly explained by the blocking versus facilitating effects as the concentration of the IL is varied. Although the diffusion should be intuitively related to the FFV, we do not find a direct correlation. This may be due to the fact that there are only very small shifts in the FFV among our systems, possibly too small to impart a change in the diffusion.

4. Conclusions

The equilibrium and transport characteristics of CO_2 in neat ionic polyimides and ionic liquid composite materials with the different IL concentrations were studied. The ILs have a plasticization effect on the i-PI, lowering the glass transition temperature (T_g) and the theoretical surface area, but the FFV is relatively constant. In general, the CO_2 solubility strongly correlates with the T_g, but the transport behavior shows a more unusual relationship with respect to the IL concentration and T_g values. At low IL concentrations, the presence of the IL tends to have a blocking effect on the CO_2 transport. However, as the IL surpasses a threshold value, a positive correlation between the IL concentration and the CO_2 diffusion begins to emerge. In general, the CO_2 molecules are strongly associated with the anion species, and as the total IL continues to increase there is a more developed anion pathway available within the system. Furthermore, the CO_2 molecules tend to diffuse via a hopping mechanism, and the higher IL concentrations decrease the T_g considerably, which is found to accelerate the void-to-void CO_2 hopping rates.

Compared to the range of different polymers reported in the literature, the diffusion coefficients in our system are approximately two orders of magnitude slower. This is likely due to rigidity of our polymer backbone. We are currently exploring other alternatives that can provide the necessary free volume for gas diffusion but are also flexible enough to allow for accelerated hopping through the polymer network. In these systems, it is important to understand the molecular-level mechanisms that are controlling the equilibrium and transport behavior, as there can be strongly non-linear relationships that emerge in these confined environments.

Supporting Information

The Supporting Information is available free of charge on the ACS Publications website at DOI: 10.1021/acs.jpcb.xxxxxx. Summary of diffusion coefficients of CO_2 in various polymer materials from the literature; RDFs between different sites of the i-PI backbone; RDFs between CO_2 and $[Tf_2N^-]$-based and $[BF_4^-]$-based polymer systems; CO_2 diffusion coefficient as a function of the i-PI+IL fractional free volume and surface area.

Acknowledgments

Support for this work was provided by the National Science Foundation (CBET-1605411) and the U.S. Department of Energy, Office of Science, Office of Basic Energy Sciences, Separation Science program under Award Number DE-SC0018181. Computer resources were provided by the Alabama Supercomputer Center.

References

1. Freeman, B. D.; Yampolskii, Y., *Membrane gas separation*. John Wiley & Son: West Sussex, 2010.
2. Bernardo, P.; Drioli, E.; Golemme, G., Membrane gas separation: a review/state of the art. *Ind. Eng. Chem. Res.* **2009,** *48*, 4638-4663.
3. Xiao, Y.; Low, B. T.; Hosseini, S. S.; Chung, T. S.; Paul, D. R. The strategies of molecular architecture and modification of polyimide-based membranes for CO2 removal from natural gas—A review. *Prog. Polym. Sci.* **2009,** *34*, 561-580.
4. Koros, W. J. In *Barrier polymers and structures: overview*, ACS Symposium series-American Chemical Society (USA), 1990.
5. Martín, C. F.; Stöckel, E.; Clowes, R.; Adams, D. J.; Cooper, A. I.; Pis, J. J.; Rubiera, F.; Pevida, C. Hypercrosslinked organic polymer networks as potential adsorbents for pre-combustion CO2 capture. *J. Mater. Chem.* **2011,** *21*, 5475-5483.
6. Baker, R. W. *Membrane technology and applications*. John Wiley & Sons: 2012.
7. Robeson, L. M. Correlation of separation factor versus permeability for polymeric membranes. *J. Membr. Sci.* **1991,** *62*, 165-185.
8. Aroon, M.; Ismail, A.; Matsuura, T.; Montazer-Rahmati, M. Performance studies of mixed matrix membranes for gas separation: a review. *Sep. Purif. Technol.* **2010,** *75*, 229-242.
9. Miyata, S.; Sato, S.; Nagai, K.; Nakagawa, T.; Kudo, K. Relationship between gas transport properties and fractional free volume determined from dielectric constant in polyimide films containing the hexafluoroisopropylidene group. *J. Appl. Polym. Sci.* **2008,** *107*, 3933-3944.
10. Kanehashi, S.; Nakagawa, T.; Nagai, K.; Duthie, X.; Kentish, S.; Stevens, G. Effects of carbon dioxide-induced plasticization on the gas transport properties of glassy polyimide membranes. *J. Membr. Sci.* **2007,** *298*, 147-155.
11. Bara, J. E.; Lessmann, S.; Gabriel, C. J.; Hatakeyama, E. S.; Noble, R. D.; Gin, D. L. Synthesis and performance of polymerizable room-temperature ionic liquids as gas separation membranes. *Ind. Eng. Chem. Res.* **2007,** *46*, 5397-5404.

12. Bara, J. E.; Hatakeyama, E. S.; Gin, D. L.; Noble, R. D. Improving CO2 permeability in polymerized room-temperature ionic liquid gas separation membranes through the formation of a solid composite with a room-temperature ionic liquid. *Polym. Adv. Technol.* **2008,** *19*, 1415-1420.
13. Freemantle, M. New horizons for ionic liquids. *Chem. Eng. News* **2001,** *79*, 21-21.
14. Vopička, O.; Hynek, V.; Friess, K.; Izák, P. Blended silicone–ionic liquid membranes: Transport properties of butan-1-ol vapor. *Eur. Polym. J.* **2010,** *46*, 123-128.
15. Izák, P.; Friess, K.; Hynek, V.; Ruth, W.; Fei, Z.; Dyson, J.; Kragl, U. Separation properties of supported ionic liquid–polydimethylsiloxane membrane in pervaporation process. *Desalination* **2009,** *241*, 182-187.
16. Izák, P.; Ruth, W.; Fei, Z.; Dyson, P. J.; Kragl, U. Selective removal of acetone and butan-1-ol from water with supported ionic liquid–polydimethylsiloxane membrane by pervaporation. *Chem. Eng. J.* **2008,** *139*, 318-321.
17. Vicent-Luna, J. M.; Luna-Triguero, A.; Calero, S. Storage and separation of carbon dioxide and methane in hydrated covalent organic frameworks. *J. Phys. Chem. C* **2016,** *120*, 23756-23762.
18. Budhathoki, S.; Shah, J. K.; Maginn, E. J. Molecular simulation study of the performance of supported ionic liquid phase materials for the separation of carbon dioxide from methane and hydrogen. *Ind. Eng. Chem. Res.* **2017,** *56*, 6775-6784.
19. Wu, N.; Ji, X.; Xie, W.; Liu, C.; Feng, X.; Lu, X. Confinement phenomenon effect on the CO2 absorption working capacity in ionic liquids immobilized into porous solid supports. *Langmuir* **2017,** *33*, 11719-11726.
20. Song, T.; Zhang, X.; Li, Y.; Jiang, K.; Zhang, S.; Cui, X.; Bai, L. Separation efficiency of CO2 in ionic liquids/poly (vinylidene fluoride) composite membrane: A molecular dynamics study. *Ind. Eng. Chem. Res.* **2019,** *58*, 6887-6898.
21. Chen, H. Z.; Li, P.; Chung, T.-S. PVDF/ionic liquid polymer blends with superior separation performance for removing CO2 from hydrogen and flue gas. *Int. J. Hydrogen Energy* **2012,** *37*, 11796-11804.
22. Ito, A.; Yasuda, T.; Yoshioka, T.; Yoshida, A.; Li, X.; Hashimoto, K.; Nagai, K.; Shibayama, M.; Watanabe, M. Sulfonated polyimide/ionic liquid composite membranes

for CO2 separation: Transport properties in relation to their nanostructures. *Macromolecules* **2018,** *51*, 7112-7120.

23. Mittenthal, M. S.; Flowers, B. S.; Bara, J. E.; Whitley, J. W.; Spear, S. K.; Roveda, J. D.; Wallace, D. A.; Shannon, M. S.; Holler, R.; Martens, R. Ionic polyimides: hybrid polymer architectures and composites with ionic liquids for advanced gas separation membranes. *Ind. Eng. Chem. Res.* **2017,** *56* , 5055-5069.

24. Duczinski, R.; Bernard, F.; Rojas, M.; Duarte, E.; Chaban, V.; Dalla Vecchia, F.; Menezes, S.; Einloft, S. Waste derived MCMRH-supported IL for CO2/CH4 separation. *J. Nat. Gas Sci. Eng.* **2018,** *54*, 54-64.

25. Dunn, C. A.; Shi, Z.; Zhou, R.; Gin, D. L.; Noble, R. D. (Cross-linked poly (ionic liquid)–ionic liquid–zeolite) mixed-matrix membranes for CO2/CH4 gas separations based on curable ionic liquid prepolymers. *Ind. Eng. Chem. Res.* **2019,** *58*, 4704-4708.

26. Li, P.; Pramoda, K.; Chung, T.-S. CO2 separation from flue gas using polyvinyl-(room temperature ionic liquid)–room temperature ionic liquid composite membranes. *Ind. Eng. Chem. Res.* **2011,** *50*, 9344-9353.

27. Kanehashi, S.; Kishida, M.; Kidesaki, T.; Shindo, R.; Sato, S.; Miyakoshi, T.; Nagai, K. CO2 separation properties of a glassy aromatic polyimide composite membranes containing high-content 1-butyl-3-methylimidazolium bis (trifluoromethylsulfonyl) imide ionic liquid. *J. Membr. Sci.* **2013,** *430*, 211-222.

28. Abedini, A.; Crabtree, E.; Bara, J. E.; Turner, C. H. Molecular simulation of ionic polyimides and composites with ionic liquids as gas-separation membranes. *Langmuir* **2017**, 11377-11389.

29. Abedini, A.; Crabtree, E.; Bara, J. E.; Turner, C. H. Molecular analysis of selective gas adsorption within composites of ionic polyimides and ionic liquids as gas separation membranes. *Chem. Phys.* **2019,** *516*, 71-83.

30. Shah, J. K.; Maginn, E. J. A general and efficient Monte Carlo method for sampling intramolecular degrees of freedom of branched and cyclic molecules. *J. Chem. Phys.* **2011,** *135*, 134121.

31. Shah, J. K.; Marin-Rimoldi, E.; Mullen, R. G.; Keene, B. P.; Khan, S.; Paluch, A. S.; Rai, N.; Romanielo, L. L.; Rosch, T. W.; Yoo, B. Cassandra: An open source Monte Carlo package for molecular simulation. *J. Comput. Chem.* **2017,** *38*, 1727-1739.

32.Van Der Spoel, D.; Lindahl, E.; Hess, B.; Groenhof, G.; Mark, A. E.; Berendsen, H. J. GROMACS: fast, flexible, and free. *J. Comput. Chem.* **2005,** *26*, 1701-1718.

33. Essmann, U.; Perera, L.; Berkowitz, M. L.; Darden, T.; Lee, H.; Pedersen, L. G. A smooth particle mesh Ewald method. *J. Chem. Phys.* **1995,** *103*, 8577-8593.

34.Hoover, W. G. Canonical dynamics: Equilibrium phase-space distributions. *Phys. Rev. A* **1985,** *31*, 1695-1697.

35. Parrinello, M.; Rahman, A. Crystal structure and pair potentials: A molecular-dynamics study. *Phys. Rev. Lett.* **1980,** *45*, 1196-1199.

36. Damm, W.; Frontera, A.; Tirado–Rives, J.; Jorgensen, W. L. OPLS all-atom force field for carbohydrates. *J. Comput. Chem.* **1997,** *18* , 1955-1970.

37. Frisch, M. J.; Trucks, G. W.; Schlegel, H. B.; Scuseria, G. E.; Robb, M. A.; Cheeseman, J. R.; Scalmani, G.; Barone, V.; Mennucci, B.; Petersson, G. A., et al. *Gaussian 09*, Gaussian, Inc.: Wallingford, CT, USA, 2009.

38. Canongia Lopes, J. N.; Deschamps, J.; Pádua, A. A. Modeling ionic liquids using a systematic all-atom force field. *J. Phys. Chem. B* **2004,** *108*, 2038-2047.

39. Canongia Lopes, J. N.; Pádua, A. A. Molecular force field for ionic liquids composed of triflate or bistriflylimide anions. *J. Phys. Chem. B* **2004,** *108*, 16893-16898.

40. Lopes, J. C.; Padua, A. A. In *Modeling ionic liquids using a systematic all-atom force field. Di-alkylimidazolium and tetra-alkylammonium cations, halide, triflate, bistrisflilamide, nitrate and hexa-flurophosphate anions*, 1st Int. Congress on Ionic Liquids (COIL), 2005.

41. Canongia Lopes, J. N.; Pádua, A. A. Molecular force field for ionic liquids III: Imidazolium, pyridinium, and phosphonium cations; chloride, bromide, and dicyanamide anions. *J. Phys. Chem. B* **2006,** *110*, 19586-19592.

42. Budhathoki, S.; Shah, J. K.; Maginn, E. J. Molecular simulation study of the solubility, diffusivity and permselectivity of pure and binary mixtures of CO2 and CH4 in the ionic liquid 1-n-butyl-3-methylimidazolium bis (trifluoromethylsulfonyl) imide. *Ind. Eng. Chem. Res.* **2015,** *54*, 8821-8828.

43. Turner, C. H.; Cooper, A.; Zhang, Z.; Shannon, M. S.; Bara, J. E. Molecular simulation of the thermophysical properties of N-functionalized alkylimidazoles. *J. Phys. Chem. B* **2012,** *116*, 6529-6535.

44. Trinh, T. T.; Vlugt, T. J.; Kjelstrup, S. Thermal conductivity of carbon dioxide from non-equilibrium molecular dynamics: A systematic study of several common force fields. *J. Chem. Phys.* **2014,** *141*, 134504.
45. Yampolskii, Y. Polymeric gas separation membranes. *Macromolecules* **2012,** *45*, 3298-3311.
46. Robeson, L. M.; Liu, Q.; Freeman, B. D.; Paul, D. R. Comparison of transport properties of rubbery and glassy polymers and the relevance to the upper bound relationship. *J. Membr. Sci.* **2015,** *476*, 421-431.
47. Gelb, L. D.; Gubbins, K.; Radhakrishnan, R.; Sliwinska-Bartkowiak, M. Phase separation in confined systems. *Rep. Prog. Phys.* **1999,** *62* , 1573.
48. O'Harra, K. E.; Kammakakam, I.; Bara, J. E.; Jackson, E. M. Understanding the effects of backbone chemistry and anion type on the structure and thermal behaviors of imidazolium polyimide-ionenes. *Polym. Int.* **2019**.
49. Soldatović, D.; Vuksanović, J.; Radović, I.; Višak, Z.; Kijevčanin, M. Excess molar volumes and viscosity behaviour of binary mixtures of aniline/or N, N-dimethylaniline with imidazolium ionic liquids having triflate or bistriflamide anion. *J. Chem. Thermodyn.* **2017,** *109*, 137-154.
50. Navia, P.; Troncoso, J.; Romaní, L. Viscosities for ionic liquid binary mixtures with a common ion. *J. Solution Chem.* **2008,** *37*, 677-688.
51. Paul, A.; Samanta, A. Free volume dependence of the internal rotation of a molecular rotor probe in room temperature ionic liquids. *J. Phys. Chem. B* **2008,** *112*, 16626-16632.
52. Paul, D. Gas sorption and transport in glassy polymers. *Ber. Bunsenges. Phys. Chem.* **1979,** *83*, 294-302.
53. Kanehashi, S.; Nagai, K. Analysis of dual-mode model parameters for gas sorption in glassy polymers. *J. Membr. Sci.* **2005,** *253*, 117-138.
54. Swaidan, R.; Ghanem, B. S.; Litwiller, E.; Pinnau, I. Pure-and mixed-gas CO2/CH4 separation properties of PIM-1 and an amidoxime-functionalized PIM-1. *J. Membr. Sci.* **2014,** *457*, 95-102.
55. Mason, C. R.; Maynard-Atem, L.; Al-Harbi, N. M.; Budd, P. M.; Bernardo, P.; Bazzarelli, F.; Clarizia, G.; Jansen, J. C. Polymer of intrinsic microporosity

incorporating thioamide functionality: preparation and gas transport properties. *Macromolecules* **2011,** *44*, 6471-6479.

56. Scovazzo, P. Determination of the upper limits, benchmarks, and critical properties for gas separations using stabilized room temperature ionic liquid membranes (SILMs) for the purpose of guiding future research. *J. Membr. Sci.* **2009,** *343*, 199-211.

57. Jindaratsamee, P.; Shimoyama, Y.; Morizaki, H.; Ito, A. Effects of temperature and anion species on CO2 permeability and CO2/N2 separation coefficient through ionic liquid membranes. *J. Chem. Thermodyn.* **2011,** *43*, 311-314.

58. Wijmans, J. G.; Baker, R. W. The solution-diffusion model: a review. *J. Membr. Sci.* **1995,** *107*, 1-21.

59. Freeman, B.; Yampolskii, Y.; Pinnau, I. *Materials science of membranes for gas and vapor separation*. John Wiley & Sons: 2006.

60. Kawakami, M.; Iwanaga, H.; Hara, Y.; Iwamoto, M.; Kagawa, S. Gas permeabilities of cellulose nitrate/poly (ethylene glycol) blend membranes. *J. Appl. Polym. Sci.* **1982,** *27*, 2387-2393.

TOC Graphic

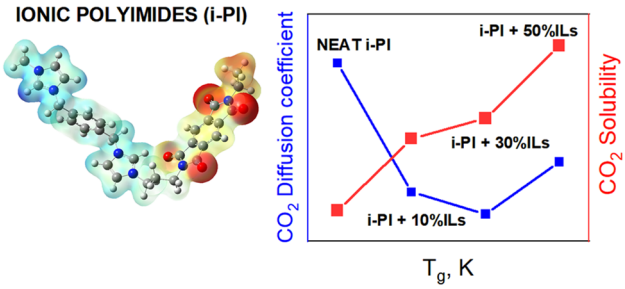
IONIC POLYIMIDES (i-PI)
NEAT i-PI
i-PI + 50%ILs
i-PI + 30%ILs
i-PI + 10%ILs
CO2 Diffusion coefficient
CO2 Solubility
Tg, K